ELSEVIER

Medical Engineering & Physics 21 (1999) 111–117

Medical Engineering & Physics

www.elsevier.com/locate/medengphy

Technical Note

Three-dimensional computational reconstruction of mixed anatomical tissues following histological preparation

S.J. Ferguson [a,c,*], J.T. Bryant [c], K. Ito [a,b]

[a] *AO ASIF Research Institute, Clavadelerstrasse, CH-7270 Davos Platz, Switzerland*
[b] *Department of Orthopedic Surgery, University of Berne, Inselspital, Berne, Switzerland*
[c] *Department of Mechanical Engineering, Queen's University, Kingston, Canada*

Received 3 July 1998; received in revised form 12 March 1999; accepted 17 March 1999

Abstract

The creation of geometrically accurate computer models of anatomical structures with complex shape and mixed tissue types can be difficult. A method for shape reconstruction based on digital images of polymer embedded, serially sectioned specimens is presented. The distortion of bone and soft tissue specimens during all stages of histological preparation was measured. Serial sections of one specimen were stained with common histological stains to enhance the contrast between different tissue types. High-resolution digital images of these sections were then processed into a three-dimensional solid model using commercial software. Preparations containing bone and cartilaginous tissues were dimensionally stable following fixation, dehydration and embedding (shrinkage/expansion less than 2%). Staining was necessary to identify anatomical features that otherwise could not be differentiated from their surroundings. Although time consuming, this method provides cross-section images of a higher resolution than those obtained from CT or MRI scanning, and with better soft tissue visualisation. © 1999 IPEM. Published by Elsevier Science Ltd. All rights reserved.

Keywords: 3D reconstruction; Anatomy; Histology

1. Introduction

In the field of biomechanics, it is necessary to create geometrically accurate computer models of anatomical objects with a higher resolution and better soft-tissue differentiation than those available with current techniques. Accurate anatomical data of objects with complex shape or composition forms the basis of computational models used in kinematic analysis and finite element analysis (FEA). Whole-joint models, which incorporate both bone and soft tissues, could be used to study the interaction of anatomical structures, for example the effect of the glenoid labrum on the stability and range of motion of the shoulder joint. Three-dimensional reconstruction from serial cross-section images is the most common technique for creating such a model. For most FEA studies based on bone anatomy, computed tomography (CT) scan datasets are used to define the model geometry. Three-dimensional models based on CT scan data have been used extensively to study the femur, pelvis and spine [1–5]. High resolution images of trabecular bone structure have been obtained using microscopic CT [6], but at present this method is limited to small specimens. The primary advantages of the CT method are: minimal distortion of the bone cross-section on the CT image, automated image processing for shape extraction, and in vivo cross-sectional data. However, it is less desirable to use CT data as the basis for models, which include structures other than bone, due to the poor resolution of soft tissues. Magnetic resonance imaging (MRI) can be used to obtain cross-sectional images with better differentiation of soft tissues [7], but the resolution of MR images is limited, typically 256 × 256 pixels. In many cases, discrete anatomical structures, such as the acetabular labrum and adjoining articular cartilage, cannot be delineated due to the ambiguous relationship between signal intensity and tissue composition [8].

Serial images of milled frozen specimens can provide high resolution images with good soft tissue visualisation [9]. However, handling and sectioning frozen speci-

* Corresponding author. Tel.: + 41-81-414-2211; fax: + 41-81-414-2288.

PII: S1350-4533(99)00032-6

mens requires specialised equipment to ensure that the specimen remains frozen throughout the process, and that a satisfactorily cut surface is obtained. Also, milling of frozen specimens unavoidably destroys the specimen. Additionally, images of the cut surface are not truly two-dimensional, as the underlying structures are visible, making evaluation more difficult. Finally, it is not possible to differentiate between similar soft tissue structures, such as the glenoid labrum and adjacent articular cartilage, the meniscus and the articular surfaces of the knee, or the acetabular cartilage layers and the acetabular labrum, due to their similar appearance on the digital images. Ideally, digital images should be obtained using a method which enhances the contrast between neighbouring soft tissue structures.

Polymer embedded specimens are routinely used in histological and gross anatomy studies to investigate the morphological properties of anatomical structures [10,11]. To make accurate morphometric measurements of tissue, it is necessary to understand the effect that specimen processing has on the dimensional distortion of the tissue. There have been numerous studies of the dimensional changes of particular tissues during histological preparation, many with conflicting results [12–16]. For example, small specimens of liver and kidney tissue shrink by up to 17% (linear) following fixation, dehydration and paraffin embedding [12], while large cancellous bone specimens may shrink by up to 7% [13]. A thickness reduction in cartilage specimens of up to 50% following histological preparation has been reported [14], but others have shown that small specimens of cartilage and subchondral bone experienced an area shrinkage of only 10% (approximately 5% linear shrinkage) following ethanol dehydration [15]. Block plastination, followed by section staining to enhance tissue contrast, has been proposed as a suitable method to study soft tissue components, such as the larynx, in their undisturbed state [16], but it is unclear whether such a procedure would be appropriate for larger specimens with a mixture of hard and soft tissues. It is to be expected that the dimensional changes of the soft tissues in such specimens would be limited by the reinforcing effect of the underlying bone. Thus, serially-sectioned, polymer-embedded specimens could provide accurate geometrical data for the three-dimensional reconstruction of hard and soft tissue anatomy.

The goal of this study was to develop a suitable method for serial specimen imaging in the special case where clear differentiation of visually similar, but compositionally different, collagenous tissues is required for large, whole-joint specimens. Preparation for imaging should not affect the dimensions of the specimen. Using this technique, it would be possible to construct accurate three-dimensional models of joints which are composed of several different tissue types, each with their own specific properties and function. This technique is demonstrated on a specimen taken from the acetabular rim, which was chosen for its variety of tissue types and composition.

2. Materials and methods

2.1. Dimensional changes

Specimens were cut from the acetabular rims of two fresh-frozen porcine hip joints using a conventional band saw (Bizerba SPA, Milan, Italy). Ovine and porcine soft tissue have mechanical properties similar to human tissue [17], and so should demonstrate similar dimensional changes during processing. Porcine specimens were selected, as they were readily available fresh from the local slaughterhouse. Specimens were taken from five different locations around the circumference of the acetabular rim. Irregularities in the cut surface were removed by grinding the specimens on a water-cooled, fine grit rotary grinding table (Struers, RotoPol-25, Copenhagen, Denmark). During preparation, the fresh specimens were kept from drying by rinsing with normal saline. The specimens were approximately 10×10 mm, 5 mm thick, and included a portion of the articular cartilage surface, the acetabular labrum, and the underlying subchondral bone (Fig. 1).

Two groups of five specimens each were prepared (unfixed, fixed). Five specimens were fixed by immersion in a 4% phosphate buffered paraformaldehyde solution for 3 days, and then rinsed with water. The five fixed specimens and the five fresh specimens were dehydrated by immersion in graded aqueous ethanol solutions of 40%, 80%, 96% and 100% ethanol for 3 days each, respectively. The specimens were then embedded following immersion in xylenol for 3 days, pure methylmethacrylate (MMA) for 3 days, MMA + 2 wt% benzoyl peroxide (b.p.) at 5°C for 3 days, and MMA + 20 vol% plasticiser + 3 wt% b.p. at room temperature until the MMA was fully polymerised. Excess MMA above the specimen surface was removed using the band saw and the rotary grinding table.

Four linear measurements and one area measurement of each specimen were taken after each stage of specimen preparation, normalised to the initial measurements of the fresh specimens. Wet specimens were measured while immersed in the appropriate preparation medium, i.e. saline or ethanol, to prevent drying. The surface of each specimen was viewed under a light microscope (WILD 308700, Heerbrugg, Switzerland) at a magnification of $\times 32$. The end points of linear measurements, and the contours of area measurements, were recorded using a digitising tablet that projected the tablet cursor onto the specimen in the microscope's field of view (Digikon 4, Kontron Electronics, Munich, Germany). Three linear dimensions of the soft tissue were recorded

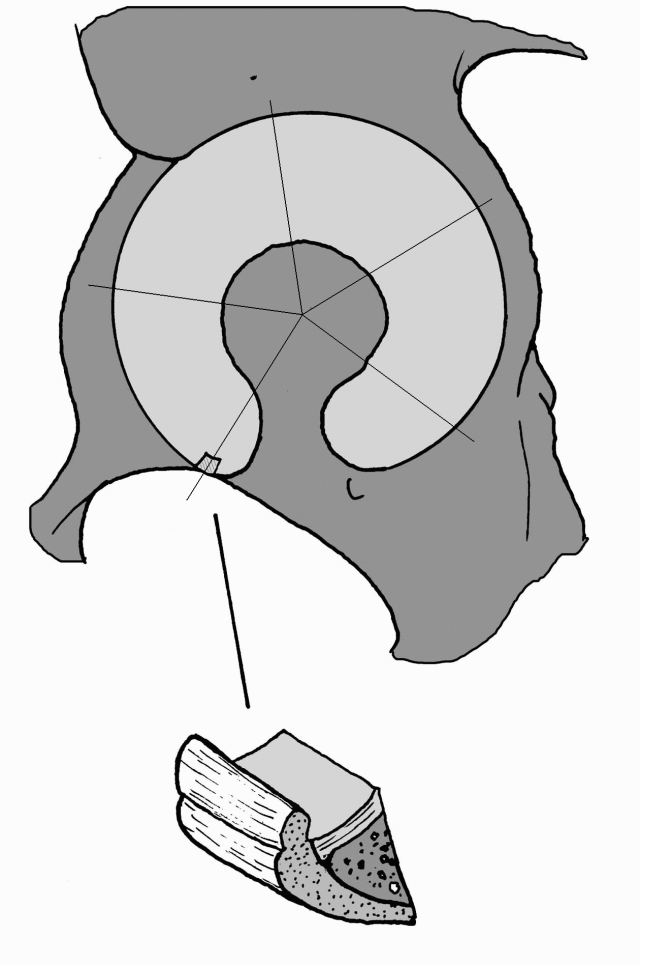

Fig. 1. Specimens for embedding and subsequent dimensional measurements were cut from five representative locations around the acetabular rim, e.g. from the inferior portion of the acetabulum near the transverse ligament. The specimens contained mixed tissue types, each with their own specific properties and function.

for each specimen using easily identified landmarks on the specimens for reference (at least one thickness measurement perpendicular to the subchondral bone and one tangential measurement along the articular surface). One linear dimension of the bone was recorded. To quantify the two-dimensional changes in specimen size, the area of a portion of the soft tissue was measured. Typical measurement locations are shown in Fig. 2. Each dimension was measured five times to evaluate errors caused by resolution limitations and operator error, and the average value was used for the calculation of dimensional changes. This series of dimension measurements was repeated after each stage of preparation (five specimens per group, five measurement locations per specimen, five repeated measurements per location). All fresh specimens were measured prior to treatment. Specimens fixed with paraformaldehyde were measured after fixation, after dehydration and after embedding in MMA. The unfixed specimens were measured after dehydration and after embedding. Out-of-plane dimension changes were assumed to be the same as the measured in-plane dimension changes.

2.2. Surface extraction

A 30 × 30 × 30 mm portion of an ovine acetabular rim was prepared as described above. The porcine specimens used for the measurement of dimensional changes were too small for meaningful 3D reconstruction. An ovine specimen was chosen to demonstrate the technique, as future projects in our lab will use a sheep model. Following embedding in methyl methacrylate, the resin block containing the specimen was ground to form two perpendicular edges for later alignment during image acquisition. The specimen was then sectioned serially, perpendicular to these two reference edges, using a diamond hole saw (Leica 1600, Leica Instruments GmbH, Nussloch, Germany), to produce 700-μm thick parallel slices 1 mm apart. Each slice was numbered, and then stained with light green, fuchsin and toluidine blue to enhance contrast between the bone, cartilage and fibrocartilage. As a staining control, several thin (6 μm) microtome sections of the same specimen were processed with a modified Movat's pentachrome stain, an excellent but more laborious differential staining technique for undecalcified, plastic-embedded thin sections [18]. The pentachrome technique is an established method which stains each tissue type with a visually distinct colour. This provided a clear reference for tissue boundaries when evaluating the quality of the proposed staining technique. The stained specimens were compared qualitatively (visually) for clear and accurate

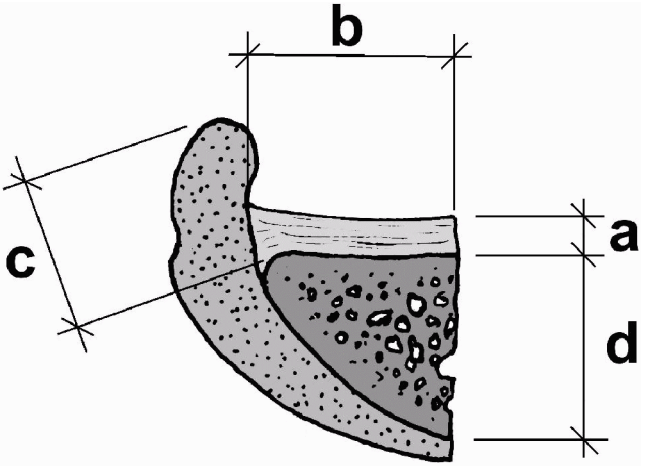

Fig. 2. Three linear soft tissue dimensions were recorded for each specimen: at least one cartilage thickness measurement perpendicular to the subchondral bone (a), one tangential measurement along the articular cartilage surface (b) and one other easily reproduced measurement within the labrum (c). One linear dimension of the subchondral bone was recorded (d), as was the area of soft tissue enclosed by a recognisable and reproducible boundary.

demarcation of tissue boundaries and colour contrast between tissue types.

Each slice was placed in an alignment frame and an image taken with a CCD digital colour camera (Sony DKC-ID1, Sony AG, Schlieren, Switzerland), 50-mm lens, with a 24-bit colour depth and at a resolution of 768 × 568 pixels, or approximately 0.05 mm/pixel. Using the SURFdriver software [19], contours were manually superimposed over the soft-tissue structures—cartilage and labrum–and the underlying bone, following visible lines of colour and tissue morphology separation. These contours were then joined by the software to form a three-dimensional surface, which could then exported to a commercial FEA software package, i.e. I-DEAS Master Series 5 (SDRC, Milford, USA).

3. Results

During the measurements, some tissue expansion and shrinkage were noticed. Considering linear dimension measurements, the unfixed soft tissue expanded, on average, by 3.5% following alcohol dehydration, and shrunk to 99.7% (± 7.8%) of its original size following polymer embedding (Fig. 3). The fixed soft tissue expanded by 5.4% following fixation, expanded a further 1.4% following dehydration, and shrunk to 100.8% (± 6.5%) of its original size following polymer embedding (Fig. 4). The dimensions of the bone tissue remained within 1.4% (± 1.8%) of their original values for both sets of specimens through all preparation steps. There was a large variance in the dimensional changes for different measuring locations. On average, there was a 1.6% standard error in the measurements of each dimension due to operator error or digitising resolution. Following polymer embedding, some tissue landmarks were not visible;

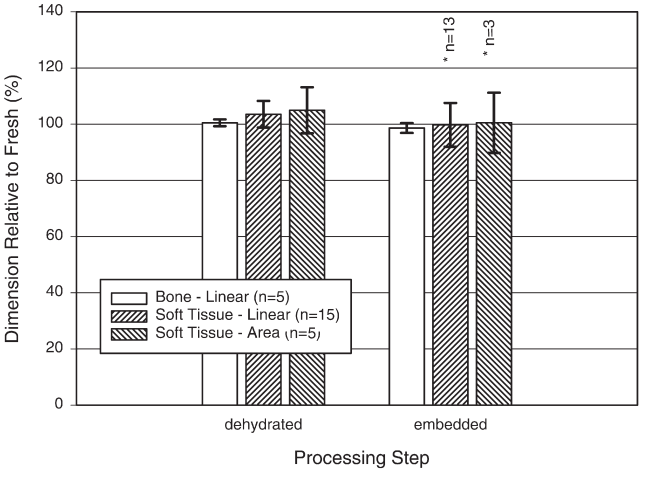

Fig. 3. In-plane dimensional changes of the specimens in the course of processing (unfixed specimens). Error bars indicate ± one standard deviation. *Polymer embedding obscured some measurement locations.

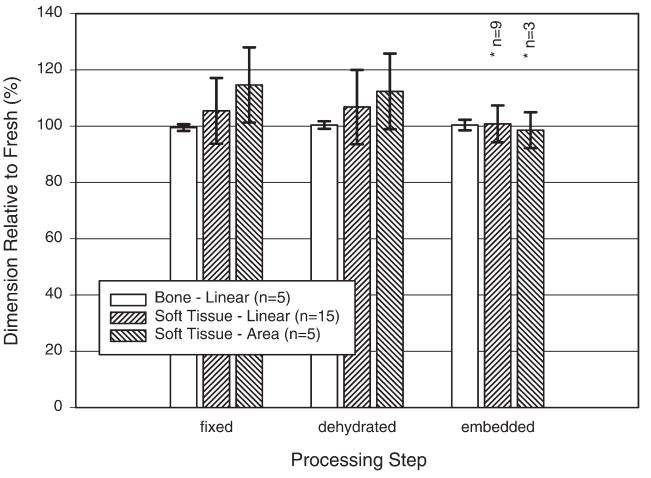

Fig. 4. In-plane dimensional changes of the specimens in the course of processing (formaldehyde fixed specimens). Error bars indicate ± one standard deviation. *Polymer embedding obscured some measurement locations.

consequently, the number of measurements for the embedded specimens was lower.

Staining with light green, fuchsin and toluidine blue enhanced the contrast between different tissue types; the mineralised bone was stained bright green, the cartilage blue to violet-blue, and the fibrous connective tissues blue-green. The fibrocartilage of the labrum could be identified as a separate tissue type from the articular cartilage by a difference in colour intensity, and the visibly different tissue morphology. The surface staining technique chosen for this study produced comparable tissue differentiation and colour contrast to the pentachrome technique. Tissue boundaries defined by the light-green/fuchsin/toluidine-blue technique coincided with those shown using the pentachrome stain. Fig. 5 shows the digital image of one slice from the inferior portion of the acetabular rim, stained to show the articular cartilage surface, the fibrocartilage at the junction of the acetabular labrum and transverse ligament, and the underlying bone. Although the software allows automatic contouring using edge detection based on colour threshold values, good results were obtained only when the user manually defined the contour edge points (Fig. 6) by following visible lines of colour and tissue morphology separation. The final three-dimensional reconstruction of the ovine acetabular rim specimen is shown in Fig. 7. The finite-element model created with the I-DEAS software from the tiled-surface object exported from SURFdriver contained approximately 4200 tetrahedral elements. Element resolution was determined by the slice thickness and the number of vertices per contour.

4. Discussion

The dimensional changes of substructures within polymer-embedded specimens have been measured. Fix-

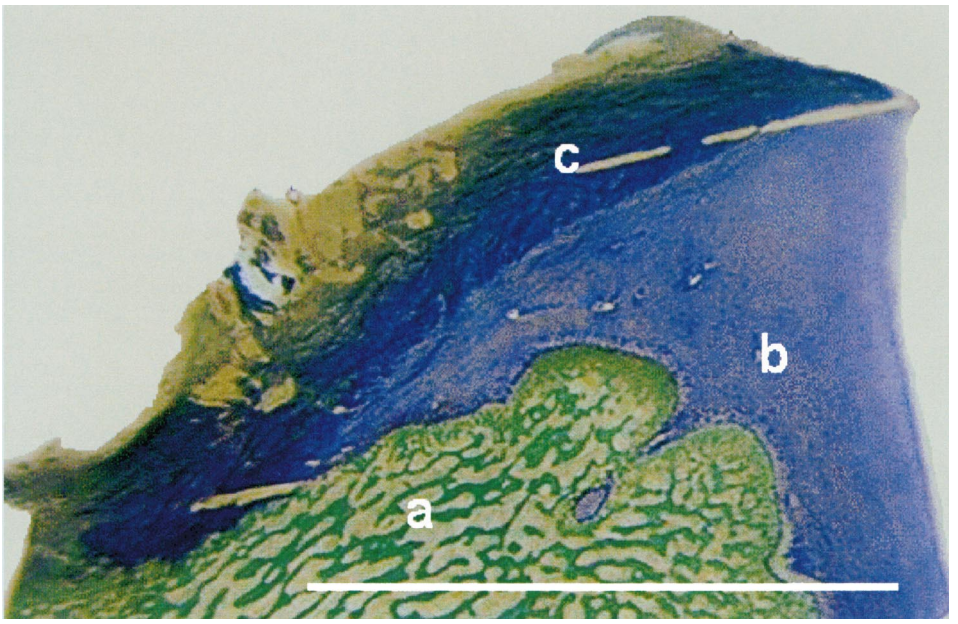

Fig. 5. A portion of one slice from the inferior portion of the ovine acetabular rim. Staining emphasises the contrast between bone (a), cartilage (b) and the fibrocartilage at the junction of the acetabular labrum and the transverse ligament (c). Scale = 10 mm.

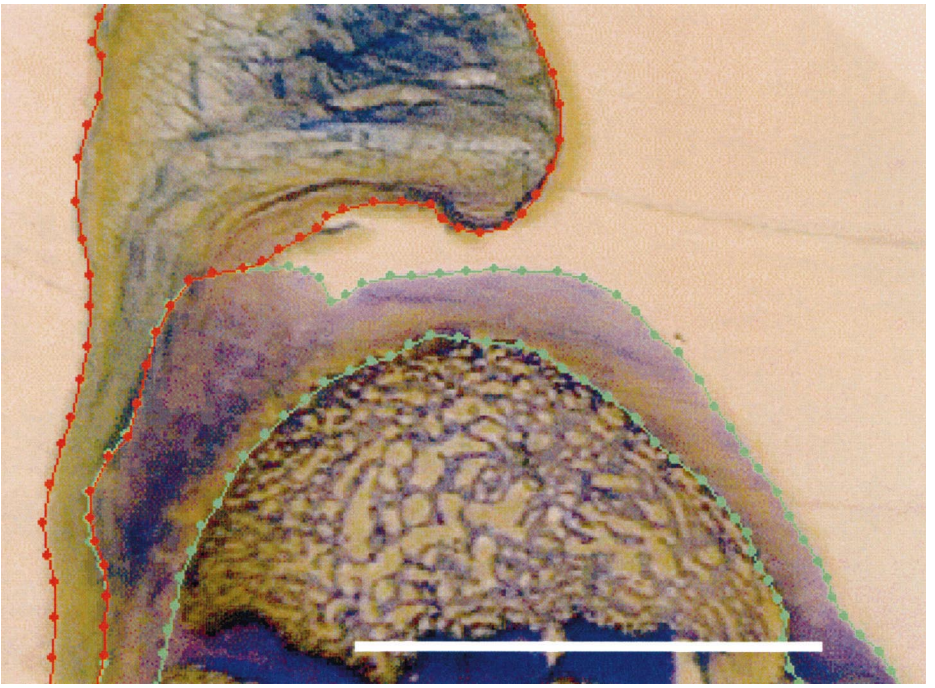

Fig. 6. Manual definition of contour vertices, using SURFdriver software, for the 3D reconstruction of a specimen cut from the acetabular rim. Tissue morphology and colour were used to determine the boundaries of individual anatomical structures. Scale = 10 mm.

ation appears to limit the extent of dimensional changes in the subsequent dehydration step. While others have reported significant shrinkage of soft tissues following dehydration and embedding, we found very little effect of the specimen preparation on final specimen size. A one-sample test to determine statistically significant differences in the dimensions of the embedded specimens relative to the fresh specimens was not performed. Due to the large standard error in the dimensional changes for different measuring locations, as indicated by the error bars in Figs. 3 and 4, compared to the small changes in the mean specimen dimensions, this statistical analysis was not necessary. Nevertheless, there is no substantial change in the specimen size after the complete preparation process. Also, as the final dimensions of the embedded specimens were distributed evenly

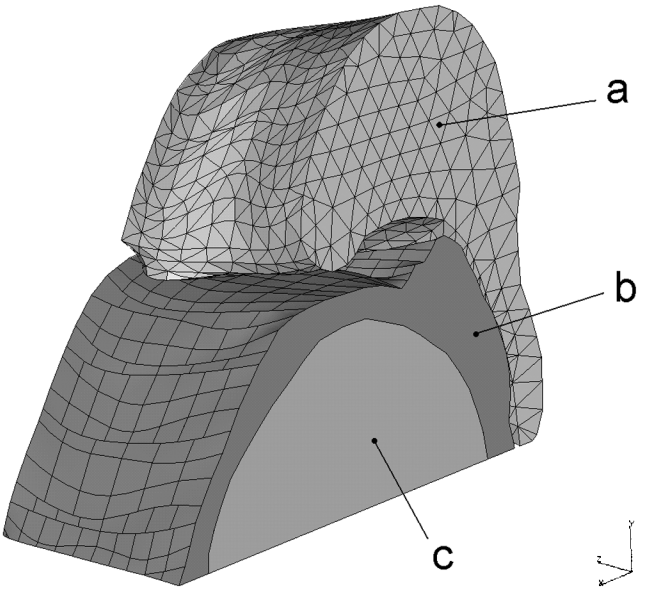

Fig. 7. The final 3D reconstruction of a specimen taken from an ovine acetabular rim, showing the fibrocartilage at the transverse ligament/labrum junction (a), the articular cartilage (b), and the subchondral bone (c). The fibrocartilage portion of the model (a) has been meshed with solid elements using I-DEAS software.

above and below the mean values of ≈ 100%, there is no tendency for tissue shrinkage or expansion. Similarly, there were no substantial differences between dimensional changes across the thickness and tangential to the articulating surface for the soft tissues. It is likely that the underlying bone reinforces the soft tissue and limits any shrinkage or expansion.

While other methods have been developed to generate cross-sectional images of anatomical structures for three-dimensional reconstruction, the method described here has certain advantages. Surface staining the specimens with light green, fuchsin and toluidine blue to enhance tissue contrast provided a means to identify the boundaries between anatomical structures that otherwise could not be seen. This is important when developing models of joints which contain visually similar, but functionally different, tissues such as the acetabular labrum and acetabular articular cartilage. For undecalcified, methacrylate-embedded specimens, the combination of light green and fuchsin, two components of the standard Goldner's trichrome stain, stains mineralised bone green and also clearly defines other tissue components, e.g. collagen, muscle and epithelia. However, the staining of cartilage is irregular and non-specific with these two, and the addition of a counterstain is required. Toluidine blue is a standard universal stain, staining non-mineralised and mineralised cartilage different shades of blue, while having virtually no effect on calcified bone. These two staining techniques are, therefore, complimentary and their combination produced the desired result for our study. Together they form a trichrome staining technique that is simple and provides a level of tissue differentiation comparable to that achieved with Movat's pentachrome stain, but with substantial time savings when processing a large number of embedded sections.

Specimens prepared by serial sectioning provide essentially two-dimensional slices, eliminating some of the ambiguity inherent when viewing the cut surface of specimens prepared using a serial milling technique. Also, using a serial sectioning process allows the specimens to be kept for further study, which is not possible with a serial milling technique, as the specimen is destroyed during processing. The resolution of the images obtained using this method is limited by the choice of digital camera; current cameras offer high resolution at a reasonable cost. An alternative method to obtain higher resolution images, at the expense of further processing time, would be to photograph each image with a standard film camera using a fine-grain film, and then scan each individual photograph with a flat-bed scanner.

The colour threshold criteria used by the SURFdriver software did not always accurately locate the boundaries between structures. The goal of this study, however, was not to specify one particular software package and segmentation technique, but rather to develop a technique for clearly differentiating visually similar mixed tissue types, and then to demonstrate a representative anatomical reconstruction. The clearly visible colour and morphology differences between tissue types made it easy to manually define smooth contours. The SURFdriver software is presented here as an option for volume segmentation and rendering. It is readily available, simple to use and economical. The additional effort of manual contour correction is offset by these factors. More advanced software packages possessing increasingly sophisticated thresholding algorithms could take advantage of the obvious colour contrast between tissue types, such that direct voxel meshing would be possible. The individual contours defined by the user were joined by the software to form a tiled surface representation of the three-dimensional geometry, which could be exported in a standard DXF or IGES format and read into a commercial FEA package, i.e. I-DEAS Master Series 5. Conversion of the tiled surface geometry to a single volume could be performed automatically in I-DEAS using the option to "stitch" all surface edges together, with only minor manual correction required by the user. The generation of a tiled surface geometry within SURFdriver produces a shape faithful to the original, but limits the possibility of mesh refinement within the FE software. Alternatively, individual contours can be exported from the segmentation software in IGES format, then used to form a solid volume by a "lofting" operation within the FE software, where a skin is drawn over the three-dimensional space defined by the cross-sectional contours. This method produces a final solid volume that

may not follow the exact shape of the original, due to smoothing, but which allows much more flexibility in the meshing operation.

5. Conclusions

A method has been presented for three-dimensional shape reconstruction based on digital images of polymer-embedded, serially-sectioned anatomical structures. Large preparations containing bone and cartilaginous tissues are dimensionally stable throughout fixation, dehydration and embedding, with linear shrinkage or expansion of less than 2% on average. Before using this method with other tissue types, the dimensional changes would have to be re-evaluated for each specific tissue type. The additional labour required for this method is offset by several advantages: high resolution images are obtained, specimens are preserved for further study, and staining can be used to enhance tissue contrast and identify anatomical features that could otherwise not be differentiated from their surroundings. This method allows a level of spatial resolution and tissue demarcation not possible with other imaging techniques, such as CT or MRI scanning, and indeed could serve as a reference standard for models created with these other techniques.

Acknowledgements

Supported in part by the AO Foundation. The authors wish to thank the following individuals for their contributions to this study: Prof. R. Ganz, I. Keller and J.-P. Imken.

References

[1] Kang YK, Park HC, Youm Y, Lee IK, Ahn MH, Ihn JC. Three dimensional shape reconstruction and finite element analysis of femur before and after the cementless type of total hip replacement. J Biomed Eng 1993;15:497–504.
[2] Keyak JH, Fourkas MG, Meagher JM, Skinner HB. Validation of an automated method of three-dimensional finite element modelling of bone. J Biomed Eng 1993;15:505–9.
[3] Merz B, Niederer P, Muller R, Ruegsegger P. Automated finite element analysis of excised human femora based on precision-QCT. J Biomech Eng 1996;118:387–90.
[4] Pfleiderer M. Micromotion of cementless acetabular cups in the pelvis (German). Ph.D. thesis, University of Hamburg-Harburg, 1997.
[5] Wu JSS, Chen JH. Clarification of the mechanical behaviour of spinal motion segments through a three-dimensional poroelastic mixed finite element model. Med Eng Phys 1996;18(3):215–24.
[6] Kuhn JL, Goldstein SA, Feldkamp LA, Goulet RW, Jesion G. Evaluation of a microcomputed tomography system to study trabecular bone structure. J Orthop Res 1990;8(6):833–42.
[7] Aritan S, Dabnichki P, Bartlett R. Program for generation of three-dimensional finite element mesh from magnetic resonance imaging scans of human limbs. Med Eng Phys 1997;19(8):681–9.
[8] Kaplan PA, Bryans KC, Davick JP, Otte M, Stinson WW, Dussault RG. MR imaging of the normal shoulder: variants and pitfalls. Radiology 1992;184(2):519–24.
[9] The visible human project. National Library of Medicine, 1998 (http://www.nlm.nih.gov/research/visible/visible_human.html).
[10] Beck JD, Keaveny TM. A serial-grinding technique for high-resolution imaging of trabecular bone. Transactions 42nd Meeting, Orthopaedic Research Society, Atlanta (GA), 1996:709.
[11] Dalstra M, Huiskes R, Van Erning L. Development and validation of a three-dimensional finite element model of the pelvic bone. J Biomech Eng 1995;117:272–8.
[12] Iwadare T, Mori H, Ishiguro K, Takeishi M. Dimensional changes of tissues in the course of processing. J Microsc 1984;136(3):323–7.
[13] Lane J, Ralis ZA. Changes in dimensions of large cancellous bone specimens during histological preparation as measured on slabs from humar femoral heads. Calcif Tissue Int 1983;34:1–4.
[14] Gilmore RSTC, Palfrey AJ. A histological study of human femoral condylar articular cartilage. J Anat 1987;155:77–85.
[15] Kaab MJ, Notzli HP, Clark J, ap Gwynn I. Dimensional changes of articular cartilage during immersion-freezing and freeze-substitution for scanning electron microscopy. Scanning Microsc, 1998.
[16] Eckel HE, Sittel C, Walger M, Sprinzi G, Koebke J. Plastination: a new approach to morphological research and instruction with excised larynges. Ann Otol Rhinol Laryngol 1993;102(9):660–5.
[17] Joshi MD, Suh J-K, Marui T, Woo SL-Y. Interspecies variation of compressive biomechanical properties of the meniscus. J Biomed Mat Res 1995;29(7):823–8.
[18] Olah AJ, Simon A, Gaudy M, Herrmann W, Schenk RK. Differential staining of calcified tissues in plastic embedded microtome sections by a modification of Movat's pentachrome stain. Stain Tech 1977;52(6):331–7.
[19] Moody D, Lozanoff S. SURFdriver, 1998 (http://surfdriver.edu.eu.org).